

Pulsed laser deposition of KNbO₃ thin films

M. J. Martín, J. E. Alfonso,^{a)} J. Mendiola, and C. Zaldo^{b)}

Instituto de Ciencia de Materiales de Madrid, Consejo Superior de Investigaciones Científicas, Cantoblanco, 28049 Madrid, Spain

D. S. Gill^{c)} and R. W. Eason

Department of Physics and Optoelectronics Research Centre, University of Southampton, Southampton SO17 1BJ, United Kingdom

P. J. Chandler

School of Mathematical and Physical Sciences, University of Sussex, Brighton BN1 9QH, United Kingdom

(Received 19 August 1996; accepted 17 March 1997)

The laser ablation of stationary KNbO₃ single crystal targets induces a Nb enrichment of the target surface. In rotated targets this effect is observed only in those areas irradiated with low laser fluence. The composition of the plasma formed close to the target surface is congruent with the target composition; however, at further distances K-deficient films are formed due to the preferential backscattering of K in the plasma. This loss may be compensated for by using K-rich ceramic targets. Best results so far have been obtained with $[K]/[Nb] = 2.85$ target composition, and crystalline KNbO₃ films are formed when heating the substrates to 650 °C. Films formed on (100)MgO single crystals are usually single phase and oriented with the (110) film plane parallel to the (100) substrate surface. (100)NbO may coexist with KNbO₃ on (100)MgO. At substrate temperatures higher than 650 °C, niobium diffuses into MgO forming Mg₄Nb₂O₉ and NbO, leading to K evaporation from the film. Films formed on (001) α -Al₂O₃ (sapphire) show the coexistence of (111), (110), and (001) orientations of KNbO₃, and the presence of NbO₂ is also observed. KNbO₃ films deposited on (001)LiNbO₃ crystallize with the (111) plane of the film parallel to the substrate surface. For the latter two substrates the Nb diffusion into the substrate is lower than in MgO and consequently the K concentration retained in the film is comparatively larger.

I. INTRODUCTION

In the last few years, increasing attention has been paid to the preparation of ferroelectric thin films. This interest is due to the possibility of producing integrated ferroelectric memories, pyroelectric sensors with fast response, miniaturized piezoelectric elements for mechanical switching and integrated optical waveguides.¹ Niobate oxides may play a major role in some of these applications and in particular the use of LiNbO₃ single crystals is widespread as a bulk optoelectronic medium, mainly due to the availability of high quality large size single crystals.² KNbO₃ is also well known for its optical properties as a photorefractive material³ and as a second harmonic generator for Al_xGa_{1-x}As diode lasers.⁴

Lithium and potassium niobate thin films have been deposited using several techniques.⁵ In particular, they

have been prepared by pulsed laser deposition on several crystalline substrates, namely LiNbO₃ on α -Al₂O₃ (sapphire)⁶ and (100)Si⁷ while KNbO₃ has been either directly deposited onto (100)MgO⁸ or by using SrTiO₃ template layers,⁹ as well as on (001)KTaO₃.¹⁰ Alkali niobate films formed from single crystal targets have an alkali metal concentration much lower than that of the target used.^{8,11} This prevents the use of dense single crystal targets and it leads to the use of ceramic targets, which in turn may increase the density of particles and target debris on the film. It is thus necessary to understand the physical origins of the K loss to minimize this effect and, if possible, use single crystal targets.

The origin of the alkali metal loss is not well understood at present. Works related to this problem are scarce. Most of the activity has been focused on LiNbO₃, but the Li concentration is difficult to calculate since it requires the use of lithium nuclear reactions.¹¹

The analysis of potassium is possible by more conventional experimental techniques, namely energy dispersive x-ray analysis (EDX) or Rutherford backscattering spectroscopy (RBS). In this work we have analyzed the target modification induced by the laser

^{a)}Permanent address: Centro Internacional de Física, Santa Fé de Bogotá, Apdo. Aéreo 49490, Colombia.

^{b)}Author to whom correspondence should be addressed.

^{c)}Present address: Foundation for Research and Technology (F.O.R.T.H.), Hellas, Institute of Electronic Structure and Laser, P.O. Box 1527, Heraklion 711 10, Greece.

ablation process, the experimental parameters leading to the niobium enrichment of the plasma and the substrate-related processes which lead to the formation of potassium deficient phases or niobium oxide segregation. It is expected that this will lead to improved pulsed laser deposition of other alkali niobates.

II. EXPERIMENTAL

Pulsed laser deposition has been performed using KrF excimer lasers (248 nm, 300 mJ/pulse). The laser beam, incident at 45°, was focused on the target which was rotated at 20 rpm in a turbopumped chamber. The laser fluence, J , on the target was measured using a Molelectron pyroelectric joulemeter. Oxygen was introduced into the chamber during film deposition. The substrate placed opposite to the target was heated either with a CO₂ laser or via resistive heating. In the first case, the substrate temperature was measured with a thermocouple glued to the back side of the substrate and in the second case it was deduced from the furnace calibration.

The composition of the targets and films was analyzed using a Philips XL-30 electron microscope equipped with EDX analysis technique which incorporates a Si(Li) x-ray detector. Typically a 5 × 5 mm² area was scanned to obtain an average value of the sample composition. RBS was also used to determine the film composition. For this purpose we use a narrow beam (1 mm²) of 1.89 MeV He ions incident at 7° (to avoid channeling of the ions), and a Si detector placed at a scattering angle of 150° to count the He ions backscattered within the surface layer. This probes to a maximum depth of 2 μm. The beam current and the total ion dose are minimized to avoid surface charge-up and accumulated ionic damage. The RBS spectra were analyzed using the RUMP software.¹²

The crystallinity and orientation of the films have been studied by x-ray diffraction using a Siemens diffractometer, model D-500, operating at the K_α emission of a Cu anode. A collimating Soller slit was used for grazing incidence x-ray diffraction (GIXRD) experiments, and removed for conventional θ -2 θ scans.

III. TARGETS

In this study we have used KNbO₃ single crystal targets grown from the melt by the top seeded solution growth technique. Moreover, K-rich ceramic targets were prepared by mixing KNbO₃ and K₂CO₃ powders in various ratios. The mixture was uniaxially pressed at room temperature up to a pressure of 200 bar to form a pellet, later dried for 4 h at 150 °C to remove the water absorbed by the hygroscopic K₂CO₃, and finally heated up to 650 °C at a rate of 5 °C/min to remove the carbon. After annealing at 650 °C, the pellets were cooled to

room temperature at 5 °C/min and subsequently stored in a dry atmosphere.

During this process, some KO₂ loss is also expected. The [K]/[Nb] composition of the targets was subsequently analyzed by EDX. Figure 1 shows the relation between the potassium-niobium ratio measured in the pellet before and after the thermal annealing at 650 °C. It is evident that the thermal treatment leads to a K loss which is necessary to fully eliminate the carbon content from the target.

The laser ablation threshold fluence, J_0 , of KNbO₃ single crystal targets has been calculated from the film thickness measured using profilometers. Using a partial oxygen pressure $P(\text{O}_2) = 2 \times 10^{-2}$ mbar, J_0 was found to be about 200 mJ/cm². A similar value was obtained for ceramic targets.

The laser ablation of KNbO₃ single crystal targets was studied by electron microscopy and EDX. Figure 2 shows the surface morphology developed in a stationary target by ablating under 2×10^{-2} mbar of oxygen pressure and using $J = 1.5$ J/cm². A homogeneous distribution of cones is observed with an average height of 100 μm. Under these conditions the average [K]/[Nb] ratio at the target surface is 0.39 and the analysis of the cone tips yields even lower [K]/[Nb] ratios, typically 0.35. Therefore, it must be concluded that potassium is preferentially ablated from the target. This preferential ablation of the target can be avoided by target rotation and increasing the laser fluence. At $J = 5$ J/cm² and $P(\text{O}_2) = 2 \times 10^{-2}$ mbar, the central part of the ablated

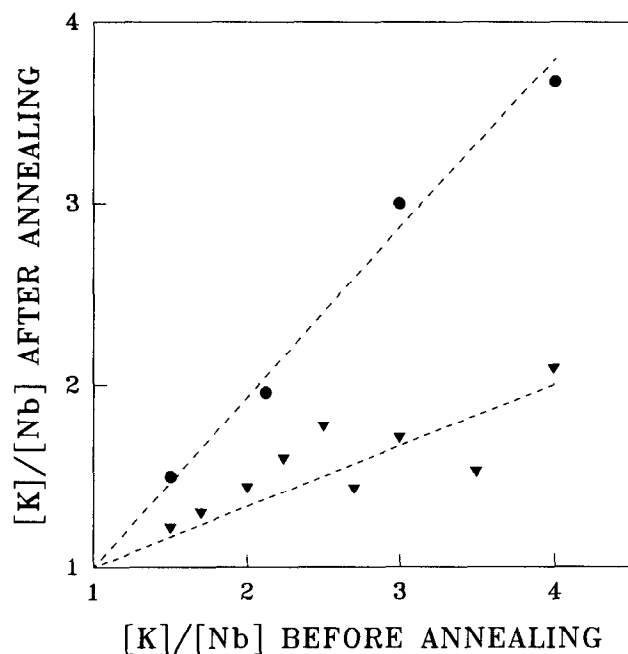


FIG. 1. Relationship between the [K]/[Nb] ratio in ceramic targets before and after the thermal annealing at 650 °C. (●) Targets annealed for 2.5 h; (▼) targets annealed for 10 h.

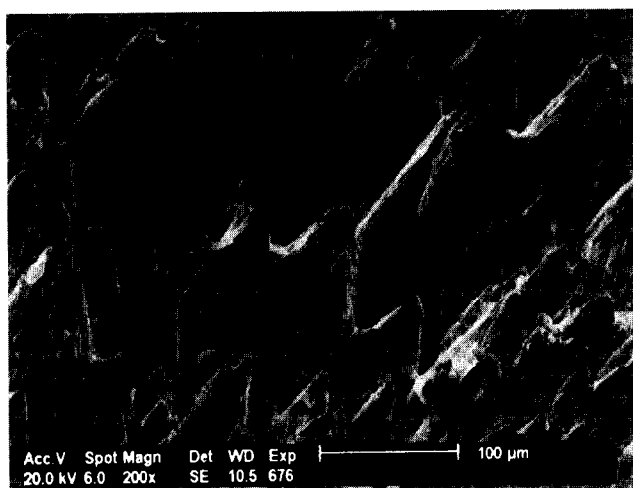


FIG. 2. Scanning electron microscopy image of the ablated surface of a single crystal KNbO₃ target. The target was ablated with 1.8×10^4 pulses at a fluence $J = 1.5 \text{ J/cm}^2$. During ablation the target was stationary.

track appears free of cones. Cones with an average height of about $20 \mu\text{m}$ are present only in the track edges. These regions correspond to the wings of the laser intensity distribution in laser pulses having low J values. The average $[\text{K}]/[\text{Nb}]$ ratio in the central part of the track has been found to be 1.1, while in the cones at the track edge the value is 0.9.

The average potassium concentration of single crystalline targets ablated at $J = 5 \text{ J/cm}^2$ is 10% larger than that found in as-grown KNbO₃ single crystals, and much higher than that found at low fluences (1.5 J/cm^2). This suggests that the laser fluence required to obtain a plasma composition congruent with the target is about 5 J/cm^2 or above. The K enrichment observed in the central part of the ablated track is likely to be due to the preferential backscattering of potassium in dense plasmas (see later).

During our thin film deposition experiments the target was always rotated and a laser fluence of 5 J/cm^2 was used; therefore the results reported above show that the K loss observed in the films may not be attributed to the modification of the target composition.

IV. THIN FILM DEPOSITION

The complex dynamics of the plasma and the substrate characteristics determine the composition and quality of the films. In what follows we will analyze some relevant processes that occur during the plasma expansion, as well as the film composition and crystalline phases formed on MgO, sapphire, and lithium niobate substrates.

Figure 3(a) shows the influence of the laser fluence on the composition of films formed on glass substrates heated to $400 \text{ }^\circ\text{C}$. The ablation of KNbO₃ single crystals produces films with $[\text{K}]/[\text{Nb}]$ ratios in the range

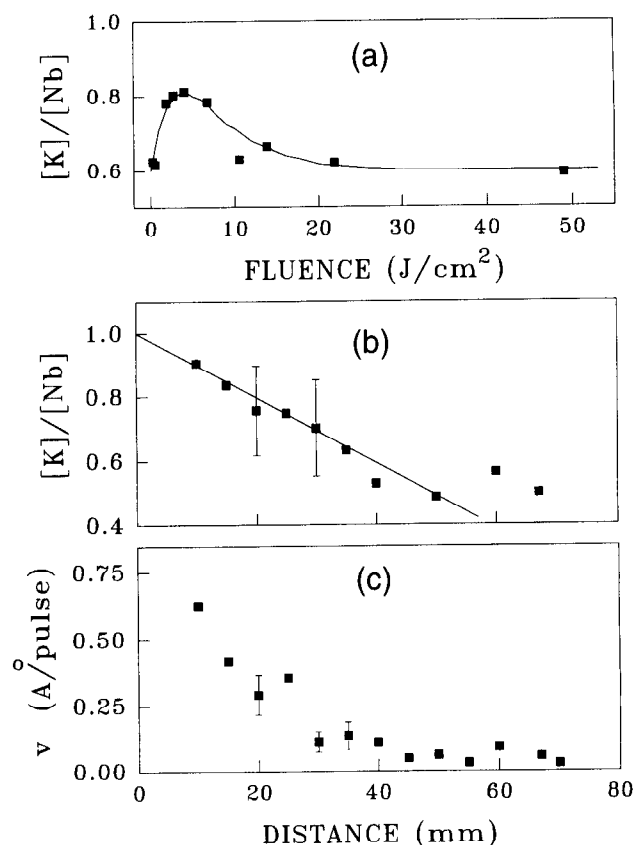


FIG. 3. (a) Variation of the $[\text{K}]/[\text{Nb}]$ ratio of films deposited by laser ablation as a function of the laser fluence. $d = 40 \text{ mm}$. (b) Variation of the $[\text{K}]/[\text{Nb}]$ ratio of films deposited by laser ablation as a function of the distance between the target and substrate. $J = 7 \text{ J/cm}^2$. (c) Variation of the growth rate, v , of films deposited by laser ablation. $J = 7 \text{ J/cm}^2$. KNbO₃ single crystal was used as target and it was ablated under an oxygen pressure $P(\text{O}_2) = 2 \times 10^{-2} \text{ mbar}$. The glass substrate was heated to $400 \text{ }^\circ\text{C}$.

0.6–0.8. As expected, films deposited are K-deficient with respect to the target. The maximum potassium concentration in the film is obtained at about $J = 5 \text{ J/cm}^2$.

The potassium concentration in the film is strongly dependent on the target-substrate distance, d . Figure 3(b) shows the $[\text{K}]/[\text{Nb}]$ ratios obtained for films deposited as a function of distance. A monotonic loss of potassium is observed with increasing distance. It is worth noting that the extrapolation to $d = 0$ suggests that the composition of the plasma at the target surface is congruent with the target but during the plasma expansion a potassium loss is produced.

According to the results above, to obtain stoichiometric KNbO₃ films a short target-substrate distance should be used. In Fig. 3(c) it is shown that this leads also to faster growth rates, but due to the limited size of the laser beam and the narrow angular spread of the plasma, the thicknesses of the films grown at short

distances are very nonuniform and therefore of limited use in most applications.

In order to further investigate the origin of the potassium loss during the plasma expansion, we have studied the influence of the oxygen pressure on the film composition. Figure 4(a) shows the $[K]/[Nb]$ ratio of films deposited on substrates placed opposite to the KNbO₃ single crystal target. As reported above, the films are K-deficient. Moreover, we have analyzed the composition of films deposited in a backscattering geometry as sketched in Fig. 4(b). For this purpose, silicon substrates were placed 15 mm off-axis from the target. Figure 4(b) shows the composition of the films formed at room temperature by the species backscattered in the plasma. These experiments have been performed by placing the substrate at several distances in the direction of the plasma expansion: only small differences in the $[K]/[Nb]$ ratio were found for the different distances used. The most important result obtained from Fig. 4(b) is that in all cases the ratio is $[K]/[Nb] > 1$, which means that potassium is more efficiently backscattered than niobium. The $P(O_2)$ dependence of the $[K]/[Nb]$ ratio in the backscattered films shows a complex behavior: At low oxygen pressures, $P(O_2) < 7 \times 10^{-3}$ mbar, the K concentration increases with pressure, followed by a decrease in the region $7 \times 10^{-3} < P(O_2) <$

1×10^{-1} mbar, and finally the K concentration increases again for $P(O_2) > 1 \times 10^{-1}$ mbar.

Some aspects of this behavior may be qualitatively understood taking into account the influence of the oxygen pressure on the plasma density and the chemical activity in the plasma. An increase of the background oxygen pressure induces an increase in the plasma density at the expanding boundary,¹³ thus increasing the collision probability of the species in the plasma. At low pressures, K and Nb should be in ionic form and the increase of the preferential backscattering of K should be related to its lower atomic mass compared with niobium, and to the increase of the collision frequency. It also seems likely that the increase of $P(O_2)$ promotes the chemical reactions in the plasma enhancing the concentration of ionic complexes or molecules among K, Nb, and O, which would equalize the K and Nb backscattering yields that in turn would maintain the K concentration in the plasma. The further increase of the relative K concentration at $P(O_2) > 10^{-1}$ mbar is not presently understood. Spectroscopic analyses of the plasma composition may lead to a better understanding of this behavior.

It is worth noting that the preferential backscattering of potassium is minimized at about $P(O_2) = 10^{-1}$ mbar. This oxygen dependence of the K concentration in the backscattered films is not the same as for the films formed at high temperature on substrates placed opposite to the target [see Fig. 4(a)]. For this geometry a smooth variation is observed. It seems likely that the K and Nb concentrations in the layer deposited on a given substrate are self-adjusted to that required to form mixed K-Nb phases.

The K deficiency in the film may be compensated by using K-rich ceramic targets. Figure 5 shows the increase of the $[K]/[Nb]$ ratio obtained using targets with increasing $[K]/[Nb]$ ratios. The K concentration of films deposited on substrates heated above 500 °C depends on the substrate nature. Films formed on MgO show a drastic decrease of the K concentration in the film (solid lines of Fig. 5); however, the $[K]/[Nb]$ ratio of films deposited on sapphire remains close to 1 even for substrate heating to 700 °C (dashed line of Fig. 5).

To further illustrate this behavior, Fig. 6 shows the RBS spectra of films deposited at high substrate temperatures on (100)MgO and (001) α -Al₂O₃. It was observed that in films deposited on MgO, the K peak decreases from 500 to 600 °C and disappears completely at 700 °C or above. Additionally, above 600 °C the peak corresponding to Nb broadens, indicative of the onset of niobium diffusion into the substrate. Figure 6 includes some of these results and the layer profiles calculated using the RUMP software. It may be observed that at 700 °C a 130 nm layer of Mg₄Nb₂O₉ is formed as well as an interdiffused region which has been simulated

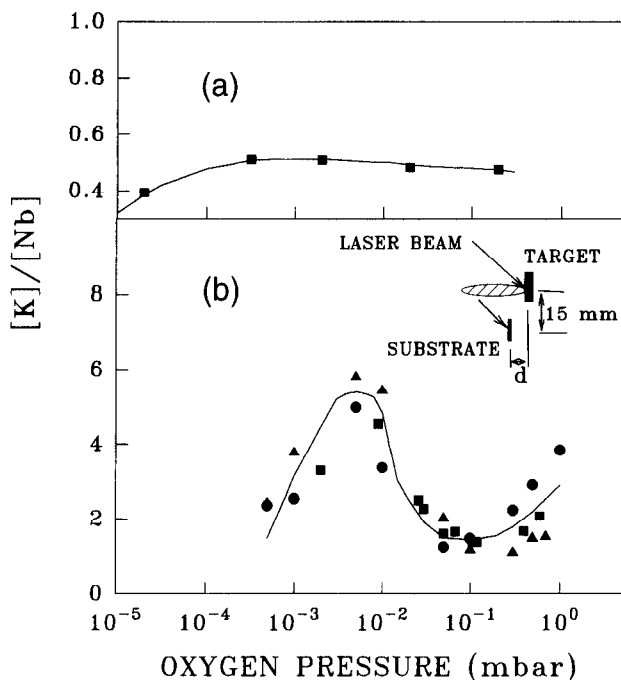


FIG. 4. Variation of the $[K]/[Nb]$ ratio of films deposited by laser ablation as a function of the oxygen partial pressure. (a) Films deposited on glass substrates placed directly opposite to a KNbO₃ single crystal target. (b) Films deposited on Si substrates placed in the backscattering configuration sketched in the figure. A KNbO₃ single crystal target was used. (●) $d = 0$ mm; (■) $d = 10$ mm; (▲) $d = 20$ mm.

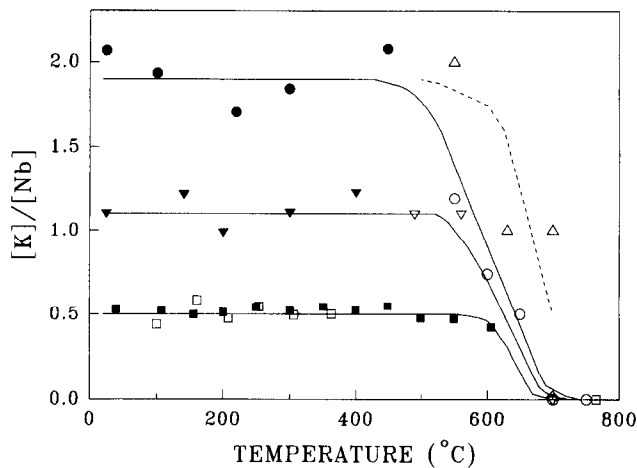


FIG. 5. $[K]/[Nb]$ ratio of films deposited by laser ablation as a function of the substrate temperature. Ceramic targets with increasing potassium concentration were used to compensate the K loss: (\square , \blacksquare) $[K]/[Nb] = 1$; (∇ , \blacktriangledown) $[K]/[Nb] = 2$; (\circ , \bullet) $[K]/[Nb] = 3.7$. Closed symbols correspond to films deposited on glass substrates and open symbols correspond to films deposited on crystalline (100)MgO substrates. (Δ) Films deposited on (001) sapphire using $[K]/[Nb] = 2.85$ ceramic targets. The lines are a guide to the eye only.

using an exponential diffusion profile with a width of $1.1 \mu\text{m}$ at $1/e$ of the maximum diffusant concentration. Heating to higher temperature, namely 800°C , the interdiffused region broadens. This case is well simulated, assuming a Gaussian diffusion profile of NbO into MgO (see the x-ray results presented later), with a maximum diffusant concentration at 200 nm below the sample surface and a full width at half of the maximum (FWHM) of $1.1 \mu\text{m}$. These results are in agreement with the previous results advanced for KNbO₃ films deposited using KNbO₃ single crystal targets.⁸

Films deposited on sapphire heated up to 700°C always show a well-resolved K peak in the RBS spectra; see Fig. 6. In addition to the top layer, these films also show an interdiffused region; however, the $1/e$ width of the exponential profiles used in the fits are more than one order of magnitude lower than in the MgO case discussed above.

These results show that the Nb diffusion in MgO is more important than in sapphire. Indeed this may be expected from the diffusion coefficients, D , reported for transition metals with ionic radius similar to Nb^{5+} ; for instance, D_{Fe} in MgO is about 10^3 times larger than in sapphire.¹⁴ The Nb diffusion into the substrate leads to a further K loss due to the low evaporation temperature of metallic potassium, namely 760°C at atmospheric pressure.¹⁵ This phenomenon may also be present in the deposition of other Na or Li oxides. Table I summarizes the evaporation temperature and the heat of vaporization for alkali metals and niobium. Inspection of Table I reveals that Nb has an evaporation temperature well above

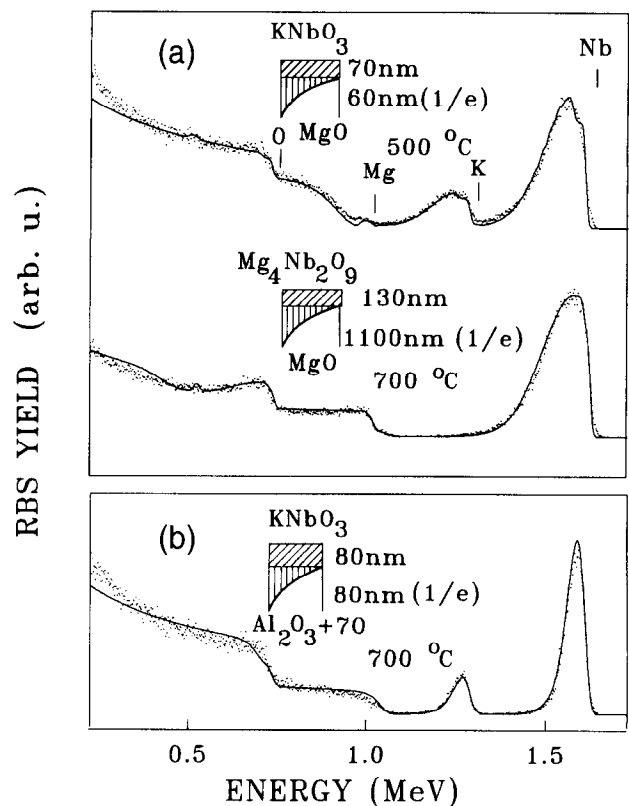


FIG. 6. Rutherford backscattering spectra of films deposited by laser ablation on (100)MgO at increasing temperatures. The experimental results are represented by dots. A $[K]/[Nb] = 2.85$ ceramic target was ablated with $J = 10 \text{ J/cm}^2$ at a $P(\text{O}_2) = 4 \times 10^{-2} \text{ mbar}$. $d = 60 \text{ nm}$. The insets sketch the diffusion profiles used for the fits, represented by solid lines. (a) (100)MgO substrates. (b) (001) sapphire substrates.

TABLE I. Evaporation temperature and heat of vaporization at ambient pressure of alkali metals and niobium.¹⁵

	Evaporation temperature ($^\circ\text{C}$)	Heat of vaporization (cal/gr)
Li	1342	5100
Na	883	1127
K	760	496
Nb	4742	

the deposition temperature used in this work. Thus its evaporation may be ignored; moreover, an increasing resistance to evaporation is evidenced going from K to Li.

Below 500°C , targets with $[K]/[Nb] = 2$ yield stoichiometric KNbO₃ films (see Fig. 5), but the films do not show a good crystalline orientation. The optimum deposition of oriented KNbO₃ on (100)MgO is obtained by a compromise between the substrate deposition temperature and the $[K]/[Nb]$ ratio of the target. On MgO substrates an incipient crystallinity is deduced from the GIXRD results of films grown at 500°C .

Optimal results have been obtained using targets with $[K]/[Nb] = 2.85$ and heating the substrate at 650 °C. Under these conditions the KNbO₃ films are usually single phase as shown previously⁸ and preferentially oriented with the [110] direction perpendicular to the substrate surface. Occasionally also a peak at 21.6° and its harmonic at 44.0° as shown in Fig. 7 are observed. They have been ascribed to the 100 and 200 diffractions of NbO present in small concentration. This phase is cubic with a lattice parameter $a = 4.212 \text{ \AA}$ ¹⁶ very close to the MgO lattice parameter, $a = 4.24 \text{ \AA}$. Therefore a very good epitaxy between both phases may be expected. Using $[K]/[Nb] = 2.85$ ceramic targets and heating the MgO substrate to about 700 °C, x-ray diffraction peaks corresponding to the Mg₄Nb₂O₉ phase appear in GIXRD scans. In good agreement with the RBS results shown above, this shows that niobium diffuses into MgO, forming a polycrystalline layer. At even higher temperature, 800 °C, the thickness of the diffused layer grows and the surface recrystallizes into a well-oriented phase responsible for an x-ray diffraction peak at 21.7°

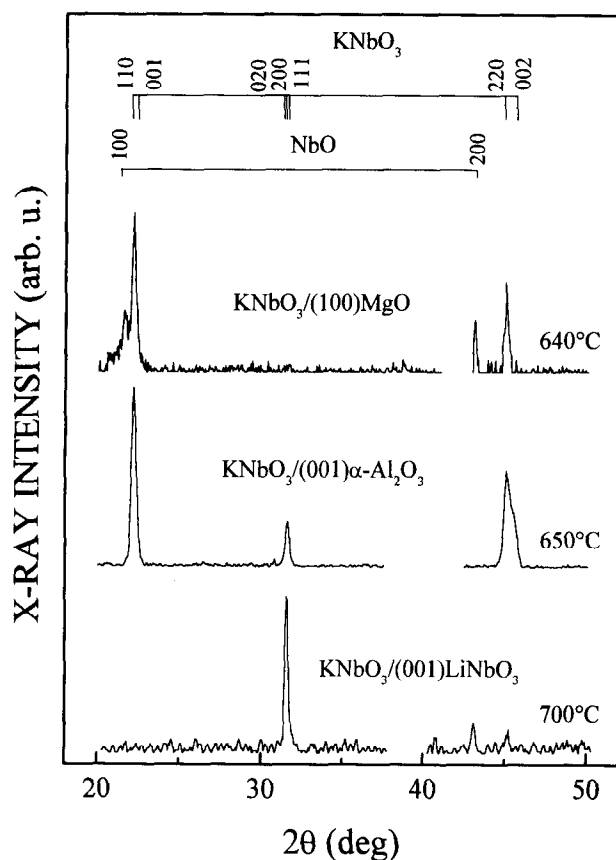


FIG. 7. θ - 2θ x-ray diffractometer scans of films deposited on (100)MgO, (001) α -Al₂O₃, and (001)LiNbO₃, heated for various temperatures. A $[K]/[Nb] = 2.85$ ceramic target was ablated with $J = 10 \text{ J/cm}^2$ at a $P(\text{O}_2) = 4 \times 10^{-2} \text{ mbar}$. $d = 60 \text{ mm}$. The diffraction peaks identified have been marked. Peaks corresponding to substrate x-ray diffraction have been removed for clarity.

observed in θ - 2θ scans. This peak is again ascribed to NbO even though now some lattice stress is likely to be present.

The pulsed laser deposition on (001) sapphire shows some differences compared to the deposition on MgO. In what follows we have used $[K]/[Nb] = 2.85$ targets and deposition conditions similar to those described above. Crystalline phases are observed only for substrate temperatures above 500 °C. Around 550 °C, two peaks at 20.7 and 41.8° appear. These peaks fit well the position corresponding to the 200 and 400 diffractions of the K₃NbO₄ phase. Simultaneously another smaller diffraction peak pair appears at 21 and 42.6°. The latter most likely corresponds to the 211 diffraction of NbO₂ and its harmonic.¹⁷ Raising the substrate temperature up to 650 °C, the K₃NbO₄ phase disappears and the KNbO₃ phase grows but several preferential orientations with the (111), (110), and (001) planes parallel to the substrate surface coexist; see Fig. 7. Raising the substrate temperature even higher, the relative contribution of the KNbO₃ (110) orientation increases, but also a larger contribution of NbO₂ is present.

The results obtained for the films deposited on sapphire have shown that Nb diffusion into the substrate is low. In these circumstances any Nb excess reaching the substrate most likely segregates as niobium oxide phases.

Figure 7 also shows the θ - 2θ x-ray diffractometer spectra obtained for films deposited on (001) LiNbO₃ substrates. As for sapphire substrates, the crystalline K₃NbO₄ phase is found in the 550–600 °C substrate temperature range. Above 650 °C KNbO₃ phase appears but now with the (111) film plane preferentially oriented parallel to the (001) lithium niobate surface.

V. SUBSTRATE-FILM EPITAXIAL RELATIONS

It is generally believed that film and substrate epitaxy requires a very good lattice match between both crystalline lattices. In semiconductor homoepitaxial films, a limited lattice parameter misfit ($\Delta a/a$) of a few percent may be accommodated by increasing the film stress.¹⁸ Increasing degrees of misfit leads to surface roughness¹⁹ and to the introduction of film defects to relieve the stress,²⁰ producing pseudoepitaxial films. In multicomponent oxides the misfit for the onset of pseudoepitaxy has been estimated to be about 3–5%.²¹ In practice, however, heteroepitaxial growth of complex oxides has been demonstrated even for lattice misfits as large as 13%.²² This may be related to the weak bonding between the film and substrate, as well as the competing island growth mechanism.

With these factors in mind, we are now in a position to discuss the experimental results concerning the film orientations found for the different substrates used.

We have found that KNbO₃ films show characteristic preferential orientations with regard to the crystalline substrates used. The (110)KNbO₃|| (100)MgO preferential growth relation has already been discussed in a previous work,⁹ and thus will not be treated further. Here we only note, however, the very good epitaxy between (100)NbO and (100)MgO lattice planes, which makes this match very likely when a K loss is induced.

Using sapphire substrates, the contributions of (111) + (110) + (001)KNbO₃|| (001) α -Al₂O₃ preferential orientations are observed, with (110) being favored at higher temperatures. Figures 8(a) and 8(b) show the atomic positional match between the *c*-oriented sapphire and the (110) and (111) lattice planes of KNbO₃. In the plot we have considered the KNbO₃ cubic phase since the deposition is performed above the tetragonal-cubic KNbO₃ phase transition temperature (428 °C). In the case of (110) preferential orientation, a good ionic match is obtained by shortening the KNbO₃ lattice by about 4% along [001] and simultaneously stretching the $[\bar{1}10]$ direction by 15.5%. In the case of (111) preferential

orientation a good match is obtained by shortening the lattice parameter of KNbO₃ by about 16%. The similarity in values of deformations of the KNbO₃ lattice required for both cases must be responsible for the observed coexistence of these film orientations.

A (111)KNbO₃|| (001)LiNbO₃ preferential orientation has also been found, as shown in Fig. 7. Figure 8(c) shows the atomic lattice match between the substrate and film planes. The ionic distribution resembles the case for *c*-oriented sapphire, but now the shortening of the KNbO₃ lattice parameter required is only 9%. This improved matching with the trigonal lattice of lithium niobate is probably the reason for the presence of a single film orientation, in contrast to films deposited on *c*-oriented sapphire substrates.

VI. CONCLUSIONS

In conclusion we have observed that two different physical processes contribute to the potassium loss, namely the preferential backscattering of potassium during the plasma expansion and the K re-evaporation from the film due to the Nb diffusion into the substrate. The potassium loss may be compensated using K-rich ceramic targets. At 650 °C, single phase KNbO₃ films, preferentially oriented along (110)KNbO₃|| (100)MgO, (111) + (110) + (001)KNbO₃|| (001) α -Al₂O₃ and (111)KNbO₃|| (001)LiNbO₃ were obtained using targets with $[K]/[Nb] = 2.85$. Above this temperature, niobium diffuses into the MgO substrate forming Mg₄Nb₂O₉, and reducing the range of deposition temperature. The Nb diffusion into sapphire and lithium niobate substrates is much lower, allowing the KNbO₃ crystallization in higher temperature. On α -Al₂O₃ the Nb excess forms NbO₂. At $T < 600$ °C the formation of the K₃NbO₄ phase on (001) α -Al₂O₃ and (001)LiNbO₃ has been observed.

ACKNOWLEDGMENTS

This work was supported by CICYT under project MAT93-0095. J. E. Alfonso was supported by a MUTIS fellowship of the Instituto de Cooperación Iberoamericana (Spain) and by COLCIENCIAS (Colombia). Thanks also to Brian Ault of the Optoelectronics Research Center, Barbara Cressey of the Geology Department of Southampton University, and to the SIDI-UAM service for the EDX analyses.

REFERENCES

1. A. Manshagh, *Ferroelectrics* **102**, 69 (1990).
2. "Properties of Lithium Niobate," EMIS Datareviews Series No. 5, INSPEC (1989).
3. P. Günter and J. P. Huignard, in *Photorefractive Materials and Their Applications I*, edited by P. Günter and J. P. Huignard (Springer-Verlag, Berlin, 1989), Chap. 2.

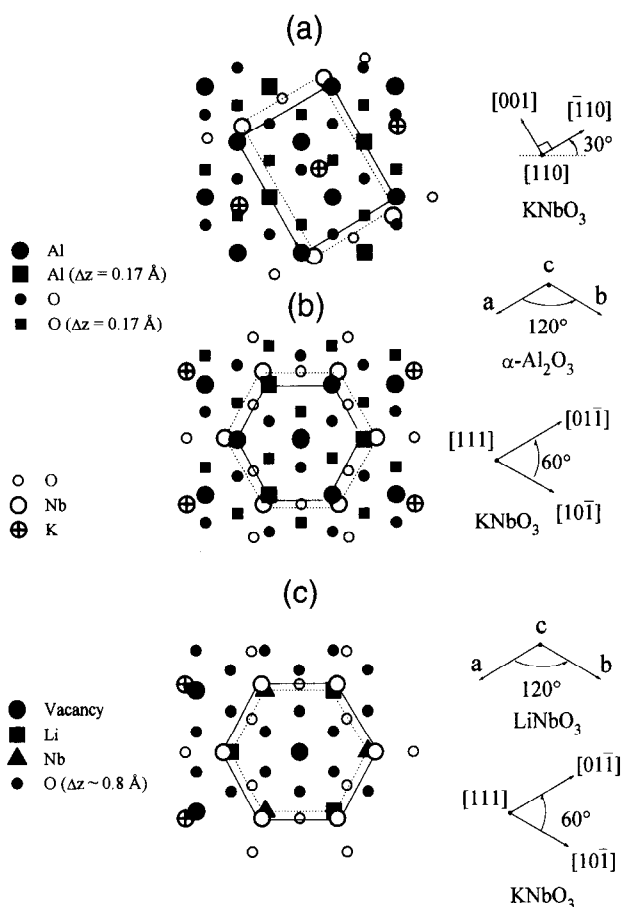


FIG. 8. (a) Projection of the ionic distribution of (001) α -Al₂O₃ and (110)KNbO₃ planes. (b) Projection of the ionic distribution of (001) α -Al₂O₃ and (111)KNbO₃ planes. (c) Projection of the ionic distribution of (001)LiNbO₃ and (111)KNbO₃ planes.

4. J. C. Baumert, P. Günter, and H. Melchior, *Opt. Commun.* **48**, 215 (1983).
5. *Handbook of Thin Film Process Technology*, edited by D. A. Glocker and S. I. Shah (IOP Publishing, Bristol, 1995), pp. X3.4 and X4.2.
6. Y. Shibata, K. Kaya, K. Akashi, M. Kanai, T. Kawai, and S. Kawai, *Jpn. J. Appl. Phys.* **32**, L745 (1993).
7. S. B. Ogale, R. Nawathey-Dikshit, and S. M. Kanetkar, *J. Appl. Phys.* **71**, 5718 (1992).
8. C. Zaldo, D. S. Gill, R. W. Eason, J. Mendiola, and P. J. Chandler, *Appl. Phys. Lett.* **65**, 502 (1994).
9. V. Gopalan and R. Raj, *J. Am. Ceram. Soc.* **78**, 1825 (1995).
10. H. M. Christen, L. A. Boatner, J. D. Budai, M. F. Chisholm, L. A. Géa, P. J. Marrero, and D. P. Norton, *Appl. Phys. Lett.* **68**, 1488 (1996).
11. C. N. Afonso, J. Gonzalo, F. Vega, E. Diéguez, J. C. Cheang Wong, C. Ortega, J. Siejka, and G. Amsel, *Appl. Phys. Lett.* **66**, 1452 (1995).
12. L. R. Doolite, *Nucl. Instrum. Methods B* **9**, 334 (1985).
13. D. B. Geohegan, in *Pulsed Laser Deposition of Thin Films*, edited by D. B. Chrisey and G. K. Hubler (John Wiley & Sons, New York, 1994), Chap. 5.
14. S. Mrowec, *Defects and Diffusion in Solids—An Introduction*, Materials Science Monographs (Elsevier, Amsterdam, 1980).
15. *Handbook of Chemistry and Physics*, 67th ed., edited by R. C. Weast (CRC Press, Boca Raton, FL, 1987).
16. A. Pialoux, M. L. Joyeux, and G. Cizeron, *J. Less-Comm. Met.* **87**, 1 (1982).
17. A. K. Cheetham and C. N. R. Raa, *Acta Crystallogr.* **32B**, 1579 (1976).
18. R. Koch, *J. Phys. Cond. Matt.* **6**, 9519 (1994).
19. A. G. Cullis, *MRS Bulletin* **21**, 21 (1996).
20. J. W. Matthews, *J. Vac. Sci. Technol.* **12**, 126 (1975).
21. Y. Y. Tomashpolsky and M. A. Sevostianov, *Ferroelectrics* **29**, 87 (1980).
22. S. Z. Wang, G. C. Xiong, Y. M. He, B. Luo, W. Su, and S. D. Yao, *Appl. Phys. Lett.* **59**, 1509 (1991).